First Stars. I. Evolution without mass loss

D. Bahena[1] • J. Klapp[2]

[1]

Abstract
The first generation of stars was formed from primordial gas. Numerical simulations suggest that the *first stars* were predominantly very massive, with typical masses $M \geq 100 M_\odot$. These stars were responsible for the reionization of the universe, the initial enrichment of the intergalactic medium with heavy elements, and other cosmological consequences. In this work, we study the structure of Zero Age Main Sequence stars for a wide mass and metallicity range and the evolution of 100, 150, 200, 250 and $300 M_\odot$ galactic and pregalactic Pop III very massive stars without mass loss, with metallicity $Z = 10^{-6}$ and 10^{-9}, respectively. Using a stellar evolution code, a system of 10 equations together with boundary conditions are solved simultaneously. For the change of chemical composition, which determines the evolution of a star, a diffusion treatment for convection and semiconvection is used. A set of 30 nuclear reactions are solved simultaneously with the stellar structure and evolution equations. Several results on the main sequence, and during the hydrogen and helium burning phases, are described. Low metallicity massive stars are hotter and more compact and luminous than their metal enriched counterparts. Due to their high temperatures, pregalactic stars activate sooner the triple alpha reaction self-producing

their own heavy elements. Both galactic and pregalactic stars are radiation pressure dominated and evolve below the Eddington luminosity limit with short lifetimes. The physical characteristics of the first stars have an important influence in predictions of the ionizing photon yields from the first luminous objects; also they develop large convective cores with important helium core masses which are important for explosion calculations.

1 Introduction

A first generation of stars composed of primordial nearly pure H/He gas must have existed, since heavy elements can only be synthesized in the interior of the stars. These *first stars*, also called Population III (or Pop III), were responsible for the initial enrichment of the intergalactic medium (IGM) with heavy elements (Bond 1981; Klapp 1981, 1983, 1984; Cayrel 1986, 1996; Carr 1987, 1994; Bromm et al. 2002).

UV photons radiated by the *first stars*, perhaps together with an early population of quasars, are expected to have contributed to the IGM reionization (Haiman and Loeb 1997; Ferrara 1998; Miralda-Escudé et al. 2000; Tumlinson and Shull 2000; Bromm et al. 2001; Schaerer 2002). The energy output from the *first stars* might have left a measurable imprint on the cosmic microwave background (CMB) on very small scales (Visniac 1987; Dodelson and Jubas 1995).

However, despite an intense observational effort, the discovery of a true Pop III remains elusive. To probe the time when star formation first started entails observing at very high redshifts $z \gtrsim 10$.

The *first stars* were typically many times more massive and luminous than the Sun (Larson and Bromm

D. Bahena

J. Klapp

[1]Astronomical Institute of the Academy of Sciences, Boční II 1401, 14131 Praha 4, Czech Republic.
e-mail: bahen@universo.com

[2]Instituto Nacional de Investigaciones Nucleares, Km 36.5 Carretera México-Toluca s/n, Salazar, Ocoyoacac, 52750 Estado de México, Mexico.
e-mail: jaime.klapp@inin.gob.mx

2004). A review of theoretical results on the formation of the *first stars* has been made by (Bromm and Larson 2004). The masses of the first star-forming clumps would have been about 500 to $1,000 M_\odot$. Several numerical simulations suggest that the *first stars* were predominantly Very Massive Stars (VMS), with typical masses $M \gtrsim 100 M_\odot$ (Bromm et al. 1999, 2002; Nakamura and Umemura 2001; Abel et al. 2000, 2002) and these stars had important effects on subsequent galaxy formation.

In another scenario, the hypothesis that *first stars* were VMS ($M > 140 M_\odot$) has been strongly criticized because the pair-instability supernovae yield patterns are incompatible with the Fe-peak and r-process abundances found in very metal poor stars. Models including Type II supernova and/or *hypernova* from zero-metallicity progenitors with $M = 8 - 40 M_\odot$ can better explain the observed trends (Tumlinson et al. 2004). The same authors also pointed out that the sole generation of VMS ($M > 140 M_\odot$) cannot be possible and suggested that some VMS could be formed as companions of stars with masses $M < 140 M_\odot$. Their Initial Mass Function (IMF) proposition match quite well with the reionization and nucleosynthesis evidence. Tegmark et al. (1997) argued that the minimum baryonic mass is redshift dependent and lies in the range $\sim 10^{3.7}$ to $10^6 M_\odot$, for $z \sim 10$ and ~ 15, respectively, and that a participation of $\sim 10^{-3}$ of the whole baryonic matter in the generation of luminous stars is sufficient to reheating the universe by $z \sim 30$.

The Wilkinson Microwave Anisotropy Probe has observed the large-angle polarization anisotropy of the CMB (Cen 2003; Kogut et al. 2003; Sokasian et al. 2003; Wyithe and Loeb 2003). Some measurements have been interpreted as a signature of a substantial early activity of massive star (MS) formation at high redshifts $z \gtrsim 15$.

The supernova explosions that ended the lives of the *first stars* were responsible for the initial enrichment of the intergalactic medium with heavy elements (Ostriker and Gnedin 1996; Gnedin and Ostriker 1997; Bromm et al. 2003; Yoshida et al. 2004). An interesting possibility unique to zero-metallicity massive stars is the complete disruption of their progenitors in pair-instability supernovae explosions, which are predicted to leave no remnant behind (Barkat et al. 1967; Ober et al. 1983; Bond et al. 1984; Fryer et al. 2001; Heger and Woosley 2002; Heger et al. 2003; Bromm and Larson 2004). The later works consider that this peculiar explosion mode could have played an important role in quickly seeding the intergalactic medium with the first metals.

Related to the *first stars*, there are two very important unsolved questions: 1. What are their typical masses and Initial Mass Function (IMF)? and, 2. During their cuasi-static evolutionary phases, do they have radiation driven winds or mass loss due to other mechanisms?

Star formation and accretion calculations suggest that the *first stars* were very massive (Omukai and Palla 2003). On the other hand, by comparing the observed abundance patterns of Extremely Metal Poor (EMP) stars with supernova explosion calculations, some authors have concluded that the *first stars* are more likely to have masses in the range $\sim 20 - 30 M_\odot$, but not more massive that $130 M_\odot$ (Umeda and Nomoto 2002; Heger and Woosley 2002).

We have suggested that a possible solution to this inconsistency is that *first stars* are born very massive but that during their cuasi-static evolutionary phases, lose mass and reach the pre-supernova stage with the masses required from supernova calculations to reproduce the EMP abundance pattern (Klapp et al. 2005; Bahena 2006). It is then very important to estimate the amount of *first stars* mass loss during the cuasi-static evolutionary phases.

Kudritzki (2000, 2002) calculated wind models of massive stars between 100 and $300 M_\odot$ and metallicities in the range 0.0001 to 1.0 solar, in an effective temperature range from $40,000$ to $60,000$ K, with the objective of predicting mass-loss rates at very low metallicities applicable to the first generation of massive stars. It was found that for very low metallicities, the line driven mechanism becomes very inefficient and wind solutions can only be obtained very close to the Eddington limit. He also pointed out that very massive stars are pulsationally unstable, which might contribute to stellar mass loss, in particular at low metallicity when the contribution of the radiative driving to the wind decreases. However, the critical mass for the onset of the nuclear pulsational instability is uncertain.

Other mechanisms could induce *first stars* mass loss, for example, the low metallicity rotation models of Meynet and Maeder (2002) show fast rotating cores that lose significant amounts of mass and thus angular momentum. Rotation by enhancing the luminosity and lowering the effective gravity increases the mass loss rate. Then, it is possible that pulsation, rotation and Luminous Blue Variables (LBV) type phenomenae could induce significant amounts of mass loss during the *first stars* cuasi-static evolutionary phases.

Motivated by the above arguments, in a series of papers we will study the structure, evolution and nucleosynthesis of the *first stars* with and without mass loss and rotation. In this Paper I we present the evolutionary results without mass loss and with no-rotation.

This work is organized as follows: In Sect. 2 we describe the initial conditions of the stellar models and

the way in which the main physical variables are computed. Then, in Sect. 3 we describe the main results, and in Sect. 4 we discuss our results and compare them with other authors. Finally, in Sect. 5 we outline our conclusions.

2 Numerical modelling and input physics

We present Zero Age Main Sequence (ZAMS) models for stars in the mass range $1 - 10,000 M_\odot$ with compositions $(X, Z) = (0.765, 10^{-2})$ for Pop I, $(X, Z) = (0.749, 10^{-3})$ for Pop II, $(X, Z) = (0.765, 10^{-6})$ for galactic Pop III, and $(X, Z) = (0.765, 10^{-9})$ and $(1.0, 10^{-10})$ for pregalactic Pop III.

In this paper, evolutionary models for Pop III stars have been calculated without mass loss and with no-rotation. The chemical composition of the models is $(X, Z) = (0.765, 10^{-6})$ and $(0.765, 10^{-9})$, for galactic and pregalactic stars, respectively. For the evolution the chosen stellar masses were 100, 150, 200, 250 and $300 M_\odot$.

The main difference between galactic and pregalactic stars is their initial metallicity. According to Castellani (2000) we consider a Pop III metallicity range from $Z = 10^{-6}$ to 10^{-10}. The transition from pregalactic to galactic stars occur at the critical metallicity $Z \sim 10^{-3.5} Z_\odot$ (Bromm and Larson 2004). Pregalactic stars are characterized by self-producing their own heavy elements; galactic stars correspond to the next generation of stars which have been previously enriched with metals.

The computer program used for the calculations has been described by Klapp (1981, 1983) and Bahena (2006, 2007), with updated input physics.

For the nuclear reaction rates we use the Nuclear Astrophysics Compilation of Reaction Rates (NACRE) by Angulo et al. (1999). A diffusion treatment for convection and semiconvection is used. For the opacity we have adopted the OPAL radiative opacities (Rogers and Iglesias 1992; Iglesias and Rogers 1993).

3 Results

3.1 Zero Age Main Sequence

For our Pop I, II and III models, in Fig. 1 we show their ZAMS Hertzsprung-Russell (HR) diagram for the mass range $1 - 10,000 M_\odot$. The objective is to understand the ZAMS structure differences as function of mass and metallicity. A large number of very detailed ZAMS models with different masses and metallicities have been calculated.

The luminosity and effective temperature increases with mass. Low mass stars are located at the right lower part of the diagram, while massive and very massive stars are found in the left upper part, because they are the most luminous and hotter. Pop III stars are hotter than their Pop I and II counterparts, and so their locus on the HR diagram is shifted to the left upper part. Pregalactic stars are bluer than galactic stars. This is shown in Fig. 1 and also in Fig. 2 that is an amplification for the $100 - 10000 M_\odot$ range. In Fig. 3 we show a log ϱ_c - log T_c diagram for a large mass and metallicity range.

In Figs. 4 to 9 we show the main physical variables for the ZAMS models. All quantities are plotted as function of the mass. As the mass increases, ZAMS stars become bigger, brighter and less dense. With decreasing metallicity, Pop III stars get very hot and compact. All massive and very massive stars are dominated by radiation pressure and develop a large convective core. In all cases, however, their luminosity is below the Eddington upper luminosity limit.

Then, we present ZAMS models in the metallicity range from $Z = 10^{-10}$ to 10^{-6} for $M = 100, 250, 500, 750$ and $1000 M_\odot$, which are shown in Figs. 10 to 15. The central density increases with decreasing metallicity. The most massive stars are less dense. MS and VMS develop a large convective core, but its size decreases slowly with decreasing metallicity. Stellar radius is lower for low-metallicity. The radius also decrease with decreasing mass, however, lower-metallicity stars are more compact. Central temperature, and effective temperature, increase with decreasing metallicity, and the most massive stars are hotter. Luminosity does not depend on metallicity but on the mass. The most massive stars are the most luminous stars. The Eddington luminosity factor $\Gamma = L/L_{edd}$, which is the ratio of the luminosity L to the Eddington luminosity L_{edd} does not depend on metallicity. The most massive stars are the ones closest to the Eddington luminosity, and the upper luminosity limit.

3.2 Stellar structure

We have calculated the evolution of 100, 150, 200, 250 and $300 M_\odot$ stars with metallicities $Z = 10^{-2}, 10^{-3}, 10^{-6}, 10^{-9}$, and 10^{-10}. Pop III stars have higher density, temperature and pressure than their Pop I and II counterparts, and are radiation pressure dominated and very luminous.

Pregalactic stars have central temperatures of about log $T_c \geq 8$ and effective temperatures of log $T_{eff} \leq 5$. A direct consequence of higher central temperatures is that they have higher energy generation rates. On the
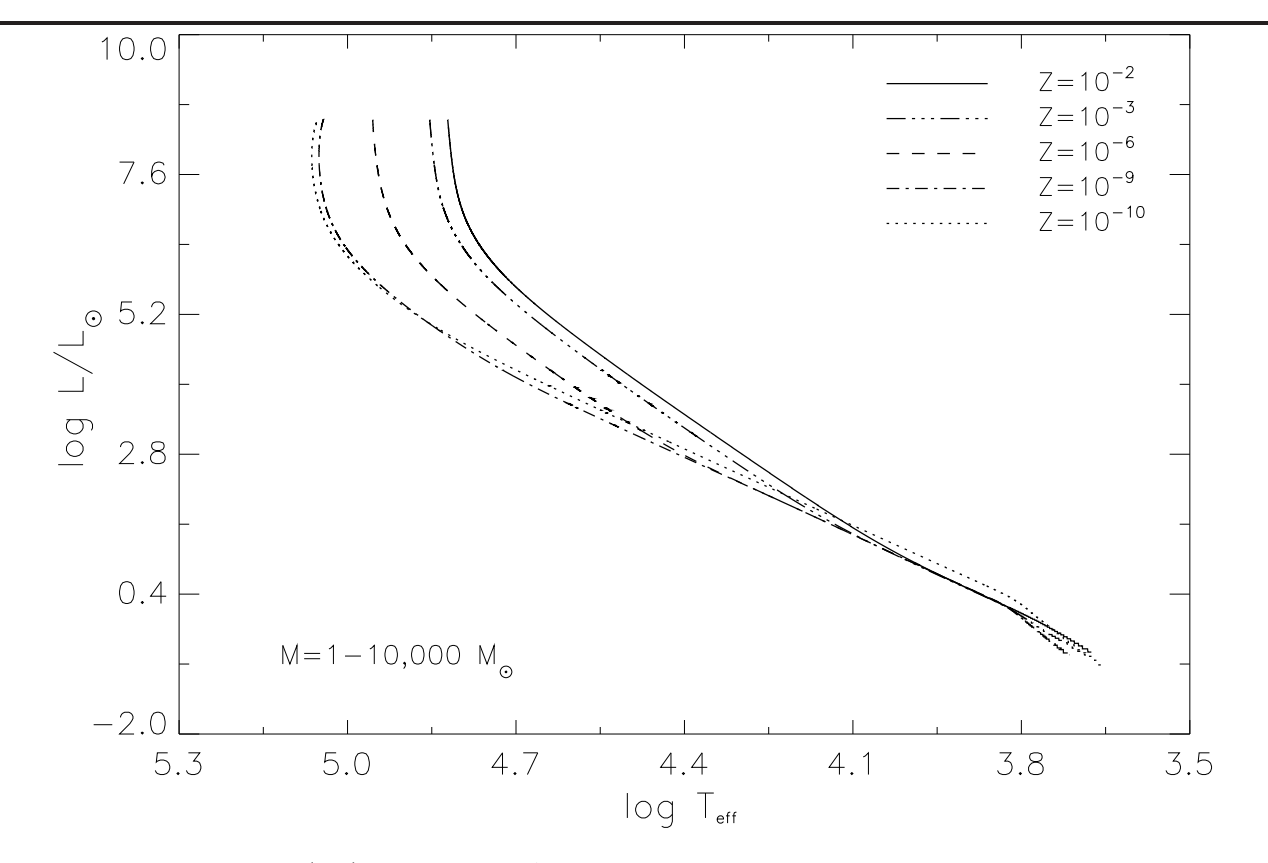
Fig. 1 Hertzsprung-Russell (HR) diagram for ZAMS Pop I, II and III stars for the mass range $1 - 10,000 M_\odot$ and metallicities $Z = 10^{-2}, 10^{-3}, 10^{-6}, 10^{-9}$ and 10^{-10}.
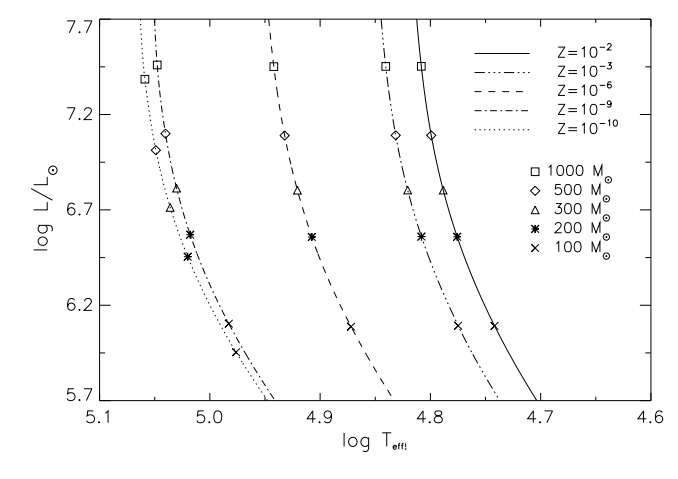

Fig. 2 HR-diagram for ZAMS Pop I, II and III stars for the mass range $100 - 10,000 M_\odot$. Depending on metallicity the Pop III ZAMS is systematically shifted to higher effective temperature.
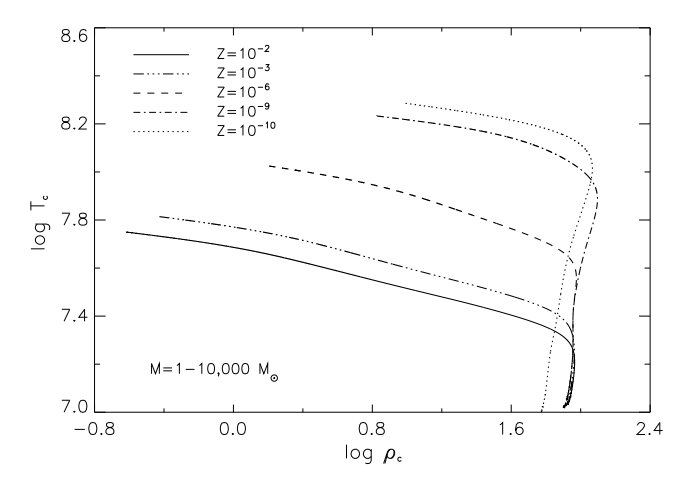

Fig. 3 ZAMS Pop I, II, and III Log ϱ_c-Log T_c plane for the mass range $1 - 10,000 M_\odot$. With increasing density and temperature, radiation pressure becomes more important.
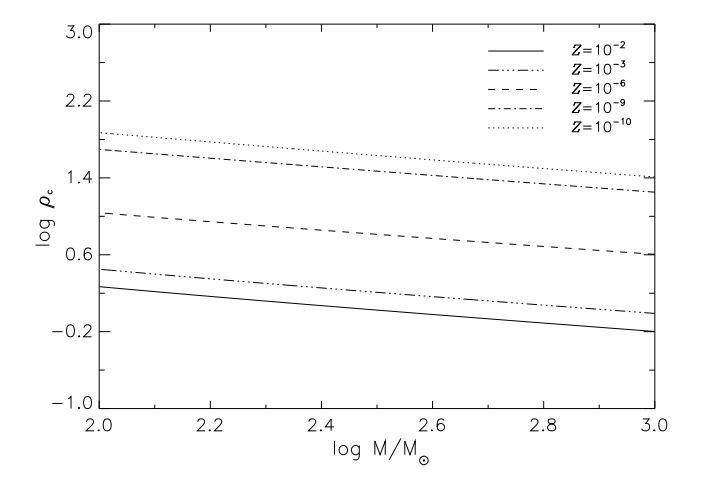
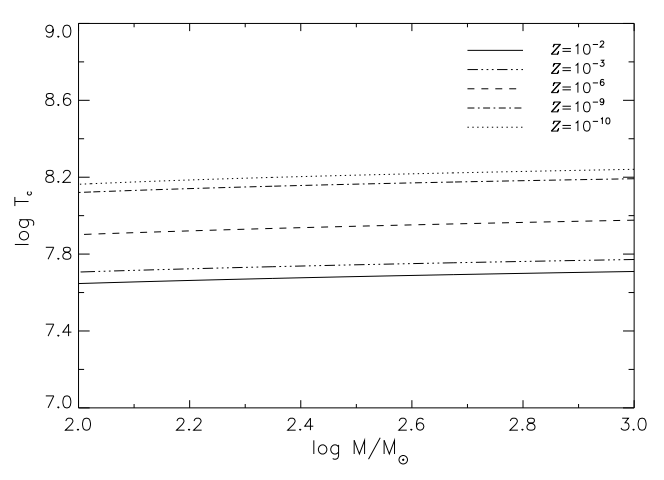**Fig. 4** Central density for ZAMS models in the mass range $1 - 10,000 M_\odot$.

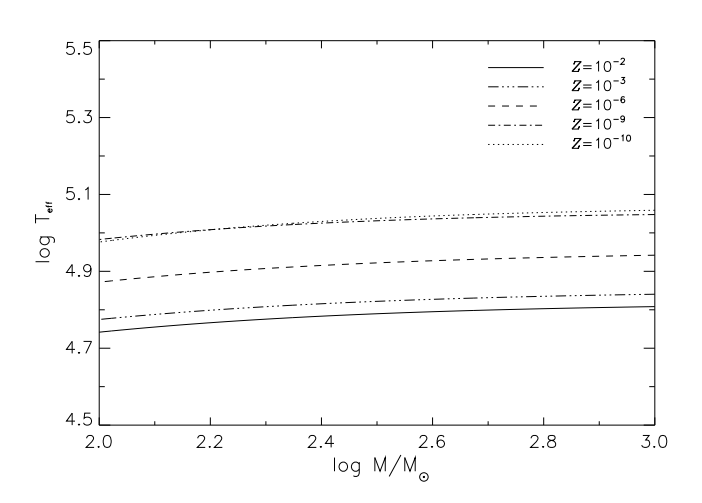**Fig. 7** *Ibidem.* Central temperature.

Fig. 5 *Ibidem.* Effective temperature.
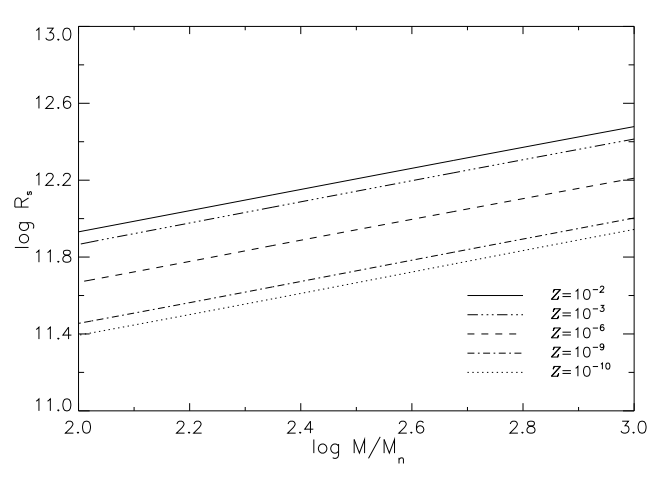

Fig. 8 *Ibidem.* Radius.
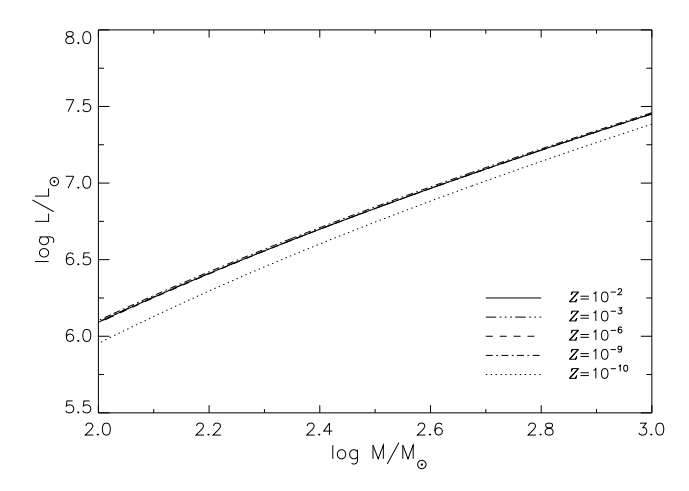
Fig. 6 *Ibidem.* Luminosity.
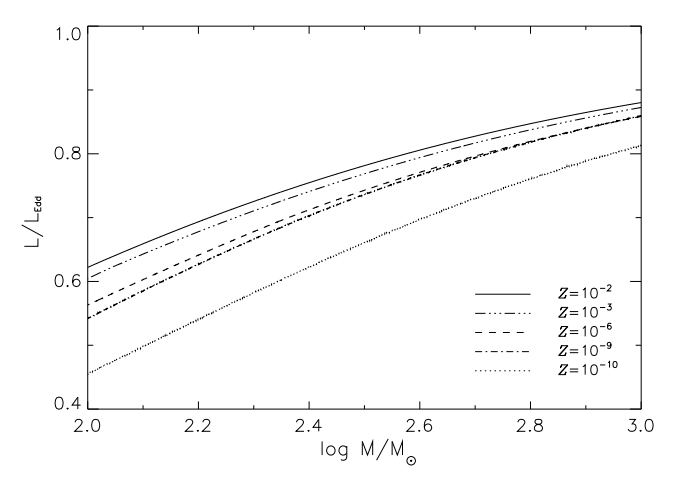
Fig. 9 *Ibidem.* Gamma factor which is the ratio of the luminosity to the Eddington Luminosity.

Fig. 10 Central density in the metallicity range from $Z = 10^{-10}$ to 10^{-6} for $M = 100, 250, 500, 750$ and $1000 M_\odot$.

Fig. 13 *Ibidem.* Central temperature.

Fig. 11 *Ibidem.* Effective temperature.
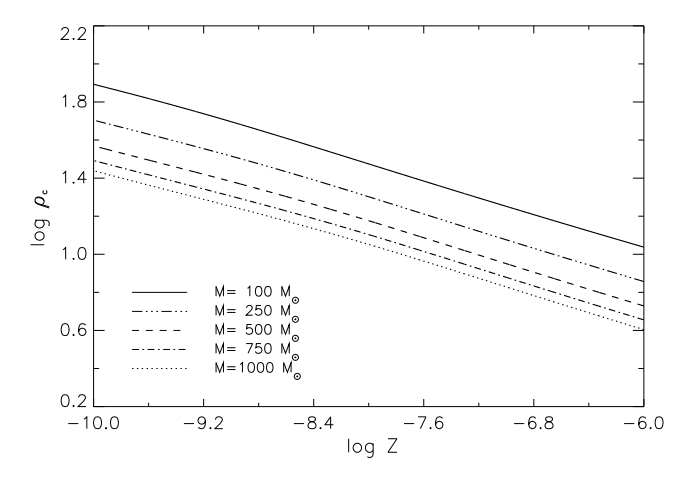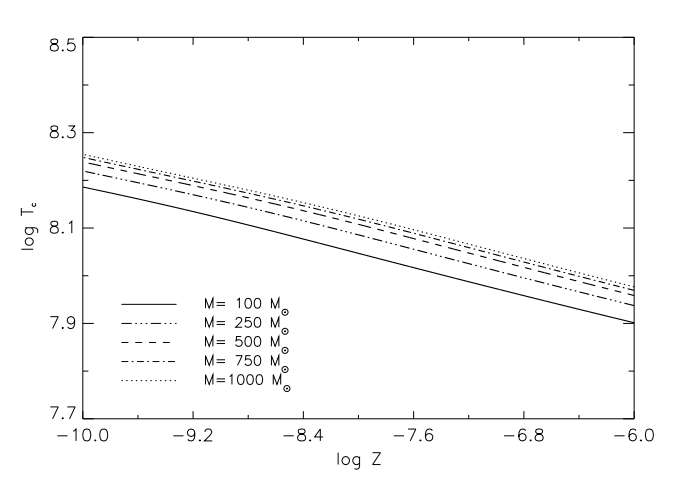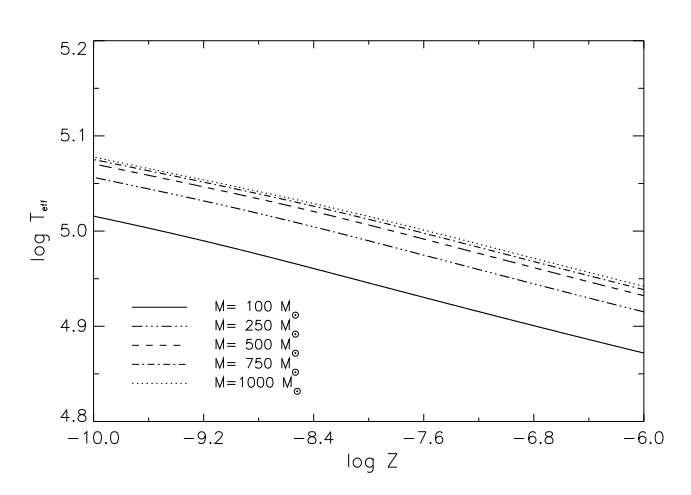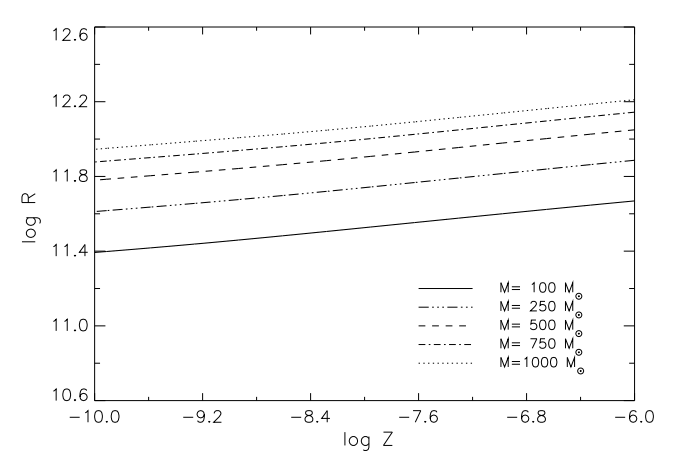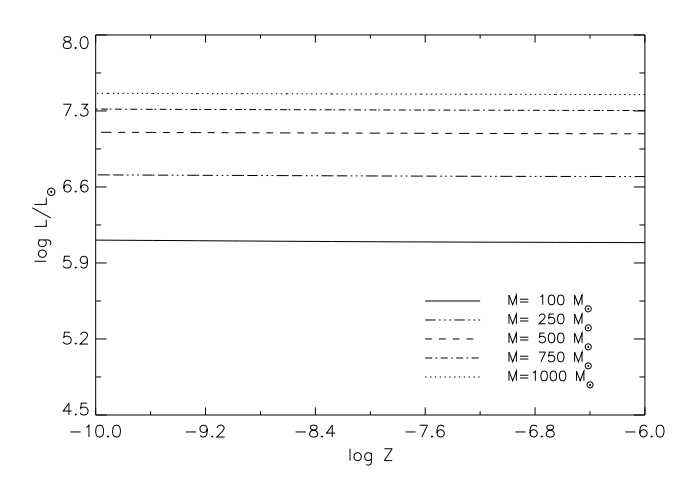

Fig. 14 *Ibidem.* Radius.

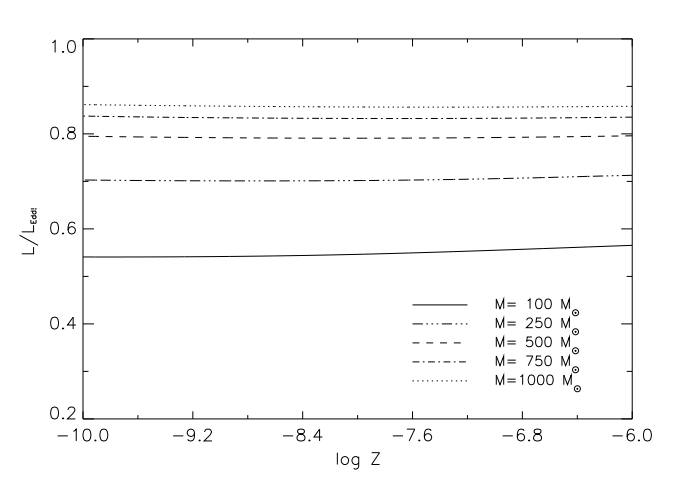**Fig. 12** *Ibidem.* Luminosity.

Fig. 15 *Ibidem.* Gamma factor.

main sequence, lower metallicity stars produce slightly less energy. However, these stars are hotter than the others and so require higher temperatures to produce the same amount of energy.

The most striking feature of the low metallicity stellar models is their atmospheric high temperature they are able to maintain. During hydrogen burning, these stars derive their nuclear energy from the inefficient pp-chains and the CNO-cycles. This is possible because a small fraction of carbon is produced during the pre-main sequence phase (Castellani et al. 1983). Some carbon is also generated by the triple-α process before the star reaches the main sequence (Bromm et al. 2001). That is, in the absence of metals nuclear burning proceeds in a non-standard way. First, the hydrogen burning occurs via the pp-chain. However, metal-free stars are hotter and very luminous reaching high central temperatures which are high enough for the simultaneous occurrence of helium burning via the triple-α reaction. After a brief initial period of this process, a trace amount of heavy metals are formed and this makes that most of the energy generation rate during hydrogen burning comes from the CNO-cycles.

Lower metallicity stars have a higher central temperature to support the star against gravity. This is a consequence of their high central density and temperature, and because this type of stars are very compact.

3.3 Stellar evolution without mass loss

3.3.1 Physical variables

For the present work stellar evolution models without mass loss have been computed during the hydrogen and helium burning phases, for very massive galactic and pregalactic Pop III $100, 150, 200, 250$ and $300M_\odot$ stars with metallicities $Z = 10^{-6}$ and 10^{-9}, respectively.

As an example of our evolution models, we list in Tables 1 and 2 some properties of $200M_\odot$ galactic and pregalactic Pop III stars.

The first two columns give the lifetime τ_6, given in units of 10^6 years, and the helium mass fraction X_{He} during the hydrogen and helium burning phases. Several physical variables in logarithmic units are included such as the central density ρ_c, the central temperature T_c, the luminosity L (in solar units), the effective temperature T_{eff}, the radius R, and the nuclear energy generation rate ϵ_{nuc}. Then, the other quantities listed are the convective core size q_{cc}, which is the ratio of the mass of the convective core to the total mass of the star, the radiation factor β_c in the centre of the star, defined by $1 - \beta = P_r/P$, where P_r is the radiation pressure and P the total pressure, and the Eddington luminosity factor Γ.

These tables summarize the most representative data of the models, and they include hydrogen and helium burning from the initial chemical composition, in 10% intervals of the helium mass fraction, to the end of helium burning when the helium mass fraction is approximately 0.01.

VMS are hot and luminous and so are located in the left upper part of the Hertzprung-Russell (HR) diagram. Because Pop III stars are hotter than their enriched counterparts, their locus in the HR-diagram is shifted to the left upper part; pregalactic stars are bluer than galactic ones.

For a given stellar mass, the evolution of a massive star, i.e., its location in the HR-diagram, depends strongly on metallicity. Metal-free stars have unique physical characteristics and they exhibit high effective temperatures and small radii. In relationship with their cosmological consequences, metal-free models are important for predicting the ionizing photon production of the first generation of stars.

Pregalactic stars were denser and hotter than galactic Pop III stars. Some of their main physical variables during the hydrogen and helium burning phases are shown in Figs.15 to 21.

The following are the main properties of the studied evolutionary models for galactic and pregalactic very massive Pop III stars.

a) Central density

Pop III stars with $Z = 10^{-6}$ settle down on the main sequence with central densities of $\rho_c = 7.46$, 5.97 and 3.94 g cm^{-3} for 100, 200 and $300M_\odot$, respectively. For the same stellar masses, and $Z = 10^{-9}$, central densities are $\rho_c = 32.18$, 29.03 and 24.83 g cm^{-3}, respectively. That is, the central density is higher for lower metallicity stars, and so, Pop III pregalactic stars are denser than galactic stars. However, the central density decreases with increasing stellar mass.

During hydrogen burning, the central density increases slowly but then by the end of this burning phase its increase rate grow significantly. The central density increases during the transition from hydrogen to helium burning and keeps increasing during the whole helium burning phase.

b) Central temperature

The VMS high energy requirements, demand high central temperatures in order to be able to maintain their structure and energy output. That is, the central temperature is high for more massive stars, but with lower metallicity the stars have an even higher temperature. At the beginning of hydrogen burning, the

Table 1 Physical variables and quantities for $200 M_\odot$ galactic Pop III stars with initial metallicity $Z = 10^{-6}$, without mass loss and with no-rotation, during the hydrogen and helium burning phases.

τ_6	X_{He}	$\log \rho_{\mathrm{c}}$	$\log T_{\mathrm{c}}$	$\log \dfrac{L}{L_\odot}$	$\log T_{\mathrm{eff}}$	$\log R$	$\log \epsilon_{\mathrm{nuc}}$	q_{cc}	β_{c}	Γ
0.04407	0.23500	0.73760	7.87567	6.55521	4.87844	11.88977	5.76058	0.89348	0.42004	0.73286
0.34457	0.30006	0.74533	7.88046	6.57138	4.87399	11.90675	5.77809	0.89744	0.40450	0.74736
0.76005	0.40003	0.76022	7.88834	6.59460	4.86358	11.93919	5.80563	0.90758	0.38060	0.77037
1.13125	0.50000	0.77986	7.89717	6.61619	4.84854	11.98007	5.83358	0.91887	0.35667	0.78979
1.46357	0.60006	0.80543	7.90722	6.63618	4.82777	12.03159	5.86349	0.92563	0.33274	0.81376
1.76063	0.70001	0.84086	7.91962	6.65458	4.80000	12.09633	5.89558	0.93542	0.30890	0.83259
2.02594	0.80008	0.89235	7.93622	6.67161	4.76299	12.17888	5.93093	0.94607	0.28509	0.85120
2.26415	0.90014	0.97789	7.96280	6.68784	4.71413	12.28471	5.96946	0.95284	0.26120	0.87436
2.46034	0.99983	1.34155	8.07854	6.70443	4.67744	12.36639	5.97202	0.46767	0.23943	0.87764
2.46037	0.99996	1.34222	8.07873	6.70444	4.67745	12.36637	5.97430	0.46771	0.23942	0.87766
2.46045	0.99986	1.34278	8.07892	6.70445	4.67745	12.36638	5.97639	0.46776	0.23942	0.87784
2.50534	0.90010	2.45172	8.42220	6.73086	4.43326	12.86797	6.41240	0.30804	0.26984	0.99198
2.52450	0.80004	2.40005	8.40679	6.73326	4.32939	13.07691	6.39498	0.40993	0.26280	0.91068
2.54783	0.70015	2.37961	8.40012	6.73469	4.24234	13.25172	6.39498	0.43042	0.25803	0.89312
2.57361	0.60009	2.37056	8.39699	6.73547	4.17638	13.38405	6.39740	0.43887	0.25356	0.88887
2.60105	0.50017	2.36860	8.39610	6.73588	4.14063	13.45575	6.40088	0.44543	0.24923	0.89512
2.62969	0.40017	2.37269	8.39710	6.73603	4.13471	13.46766	6.40352	0.45009	0.24500	0.89164
2.65913	0.30001	2.38339	8.40015	6.73596	4.14619	13.44467	6.40307	0.45347	0.24090	0.89055
2.68881	0.20014	2.40316	8.40603	6.73581	4.15927	13.41843	6.40012	0.45335	0.23697	0.88681
2.71795	0.10005	2.44120	8.41767	6.73569	4.16384	13.40923	6.36450	0.45693	0.23337	0.88916
2.73912	0.01070	2.51746	8.44134	6.73582	4.15837	13.42023	5.91299	0.45401	0.23109	0.88956
2.74053	0.00123	2.53190	8.44585	6.73588	4.15804	13.42092	5.50297	0.45446	0.23099	0.89017

Table 2 Physical variables and quantities for $200 M_\odot$ pregalactic Pop III stars with initial metallicity $Z = 10^{-9}$, without mass loss and with no-rotation, during the hydrogen and helium burning phases.

| τ_6	X_{He}	$\log \rho_{\mathrm{c}}$	$\log T_{\mathrm{c}}$	$\log \dfrac{L}{L_\odot}$	$\log T_{\mathrm{eff}}$	$\log R$	$\log \epsilon_{\mathrm{nuc}}$	q_{cc}	β_{c}	Γ
0.04407	0.23500	1.46281	8.11724	6.56930	5.00039	11.65293	5.68780	0.87527	0.42049	0.73962
0.32884	0.30008	1.47318	8.12283	6.58481	4.99569	11.67006	5.70573	0.88415	0.40503	0.75446
0.72025	0.40000	1.49258	8.13204	6.60693	4.98487	11.70278	5.73226	0.75495	0.38138	0.77484
1.06814	0.50003	1.51732	8.14230	6.62713	4.96938	11.74386	5.75997	0.90139	0.35781	0.79531
1.37810	0.60005	1.54912	8.15406	6.64545	4.94843	11.79492	5.78962	0.64234	0.33438	0.81714
1.65450	0.70003	1.59211	8.16853	6.66204	4.92085	11.85836	5.82162	0.91933	0.31113	0.83462
1.90105	0.80005	1.65303	8.18772	6.67699	4.88498	11.93759	5.85683	0.93180	0.28799	0.85101
2.11975	0.90016	1.75252	8.21821	6.69054	4.83938	12.03556	5.89503	0.93966	0.26493	0.87007
2.30096	0.99992	2.19813	8.35947	6.70693	4.80493	12.11265	5.73874	0.41750	0.24530	0.85123
2.30098	1.00006	2.19971	8.35997	6.70695	4.80505	12.11242	5.74387	0.41763	0.24533	0.85064
2.30103	0.99994	2.20122	8.36047	6.70697	4.80517	12.11221	5.74887	0.41776	0.24534	0.85011
2.32034	0.90054	2.40066	8.42261	6.71089	4.80396	12.11658	6.36513	0.41280	0.24675	0.88169
2.33776	0.80019	2.35674	8.40641	6.71097	4.78656	12.15143	6.34291	0.42242	0.24439	0.87961
2.35934	0.70013	2.34010	8.39941	6.71137	4.77235	12.18005	6.34426	0.42915	0.24187	0.87765
2.38348	0.60006	2.33432	8.39608	6.71175	4.76042	12.20409	6.34729	0.43179	0.23922	0.87840
2.40920	0.50011	2.33553	8.39510	6.71207	4.75027	12.22454	6.35226	0.43465	0.23647	0.88157
2.43607	0.40027	2.34233	8.39598	6.71239	4.74112	12.24300	6.35622	0.43754	0.23367	0.88169
2.46378	0.30015	2.35559	8.39895	6.71276	4.73206	12.26131	6.35760	0.44051	0.23084	0.88270
2.49173	0.20016	2.37737	8.40467	6.71329	4.72292	12.27985	6.34892	0.43961	0.22803	0.88389
2.51901	0.10025	2.41608	8.41584	6.71408	4.71410	12.29789	6.31307	0.43980	0.22538	0.88633
2.53894	0.01019	2.48863	8.43781	6.71513	4.70969	12.30723	5.81421	0.43147	0.22366	0.88707
2.53997	0.00157	2.49814	8.44068	6.71524	4.70981	12.30705	5.86620	0.43179	0.22360	0.88798
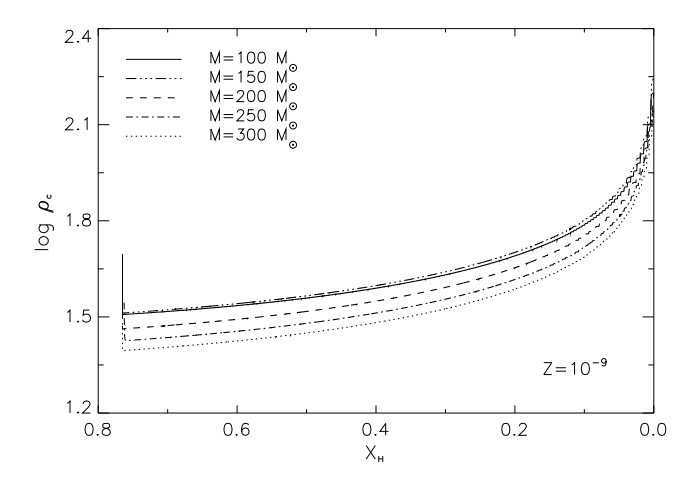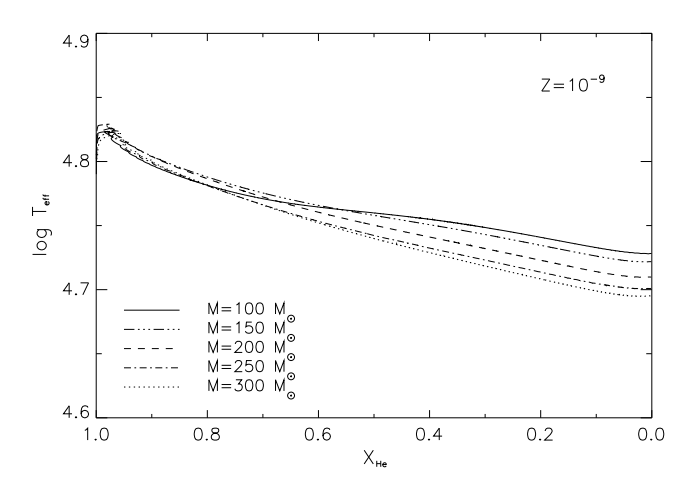
Fig. 16 Central density for $100 M_\odot$ (solid line), $150 M_\odot$ (dash-dot-dot-dot-dash), $200 M_\odot$ (dashes), $250 M_\odot$ (dash-dot-dash) and $300 M_\odot$ (dots) pregalactic Pop III stars with metallicity $Z = 10^{-9}$, without mass loss, during the hydrogen burning.

Fig. 19 Central density for $100 M_\odot$ (solid line), $150 M_\odot$ (dash-dot-dot-dot-dash), $200 M_\odot$ (dashes), $250 M_\odot$ (dash-dot-dash) and $300 M_\odot$ (dots) pregalactic Pop III stars with metallicity $Z = 10^{-9}$, without mass loss, during the helium burning phase.
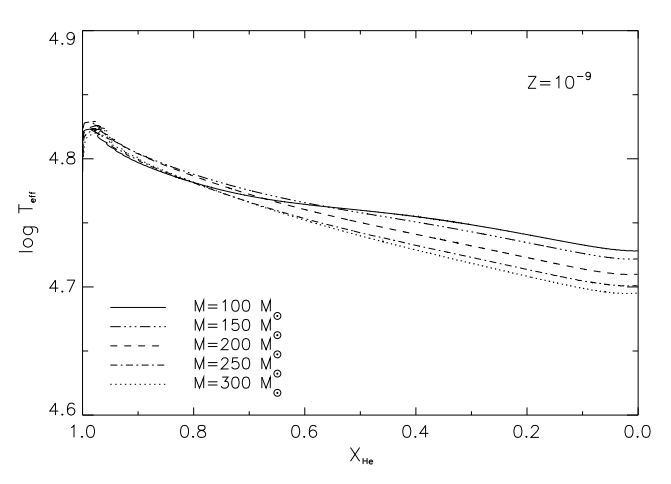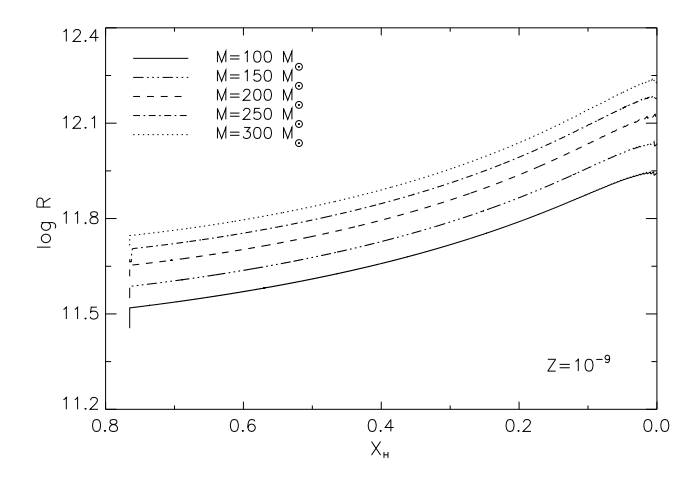

Fig. 17 *Ibidem.* Effective temperature.

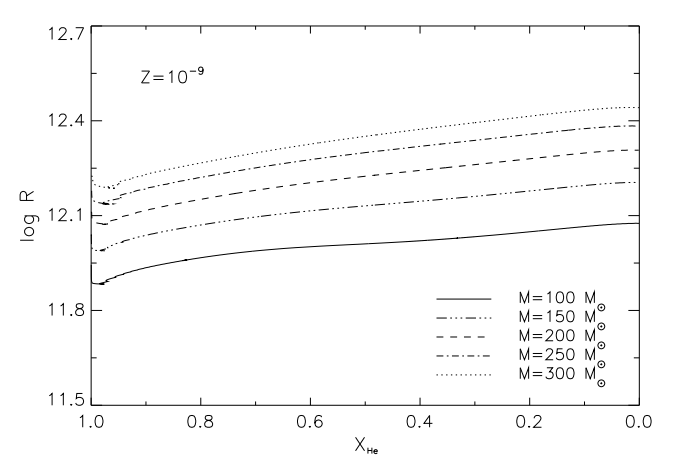**Fig. 20** *Ibidem.* Effective temperature.

Fig. 18 *Ibidem.* Radius.

Fig. 21 *Ibidem.* Radius.

central temperature with $Z = 10^{-6}$ is $T_7 = 7.02$, 7.51 and 7.76, for 100, 200 and $300 M_\odot$ stars, respectively, where $T_n = T/10^n$ K. For $Z = 10^{-9}$, the corresponding temperatures are $T_8 = 1.14$, 1.30 and 1.36, respectively. During hydrogen burning, T_c slowly increases until the end of this burning phase when it begins to increase to high values and continues to do so during the whole helium burning phase.

c) Nuclear energy generation

During hydrogen burning the main energy source is given by the CNO-cycles because of their strong temperature dependence. In lower metallicity stars these cycles are activated just after a short helium burning phase that produces enough CNO elements for the CNO-cycles to operate.

With increasing stellar mass, the central temperature is higher and so the nuclear energy generation. However, for pregalactic stars it increases with decreasing metallicity. As a consequence of the larger central temperatures, CNO-cycles carbon production is enhanced at an earlier evolutionary phase than in less massive stars. The nuclear energy generation increases during hydrogen burning. But, for galactic Pop III stars with metallicity $Z = 10^{-6}$, the energy generation rate decreases when hydrogen tends to be exhausted. When the existing hydrogen mass fraction is about ~ 0.02, and the helium mass fraction reaches ~ 0.98, the nuclear energy generation decreases. For pregalactic stars with $Z = 10^{-9}$, during the transition from hydrogen to helium burning there is only a small decrease in the nuclear energy generation rate, i.e. the transition from hydrogen to helium burning is smooth, quite different than for galactic stars.

There are different nuclear generation rates at the end of hydrogen burning because the central temperature in galactic Pop III stars is not high enough for helium ignition. This situation does not take place in the case of pregalactic stars precisely because they have a higher central temperature at the end of hydrogen burning. Then, the transition to the next burning phase occurs in a smoother form. In the other case, a strong explosive helium flash takes place during the transition to helium burning. At this moment, the star is contracting, consequently, it is heated and reaches an appropriate central temperature to ignite helium.

When helium is ignited in the core of the star, the nuclear energy generation rate increases rapidly during the transition to helium burning, then reaches a maximum and decreases towards the end of this burning phase. This occurs for galactic stars with metallicity $Z = 10^{-6}$. In the case of pregalactic stars, with metallicity $Z = 10^{-9}$, this transition takes place very smoothly because the stars are hot enough to ignite helium immediately after exhausting hydrogen. Then the generation rate increases towards a maximum and decreases by the end of helium burning.

d) Luminosity

Very massive Pop III stars are very luminous. For 100, 200 and $300 M_\odot$ with metallicity $Z = 10^{-6}$, at the beginning of the main sequence, their luminosity are $L = 1.22 \times 10^6$, 3.59×10^6 and $6.31 \times 10^6 L_\odot$, respectively. For stars with $Z = 10^{-9}$, the corresponding figures are $L = 1.27 \times 10^6$, 3.71×10^6 and $6.51 \times 10^6 L_\odot$. During hydrogen burning the stellar luminosity increases slightly and varies smoothly during the transition from hydrogen to helium burning. Then it remains practically constant during helium burning.

e) Effective temperature

Pregalactic Pop III stars are hotter than galactic stars. At the beginning of the main sequence, galactic stars with $Z = 10^{-6}$ have an effective temperature $T_{\text{eff}} = 69582$, 75586 and 77988 K for 100, 200 and $300 M_\odot$, respectively. For the same stellar masses, pregalactic stars with $Z = 10^{-9}$ have $T_{\text{eff}} = 89170$, 100090 and 103390 K, respectively. These different values are due to their higher central temperatures and the different mechanisms to drive nuclear burning.

The effective temperature continuously decrease during hydrogen burning, until the transition to helium burning that it increases. Then, the effective temperature start to decrease but then remains practically constant until the end of this burning phase when the effective temperature decreases even more.

f) Radius

Very massive Pop III stars are compact. On the main sequence, galactic stars with metallicity $Z = 10^{-6}$ have initial radii $R = 7.67$, 11.15 and $13.88 R_\odot$ for 100, 200 and $300 M_\odot$, respectively. For pregalactic stars with $Z = 10^{-9}$, their radii are $R = 4.75$, 6.46 and $8.02 R_\odot$, respectively.

As the effective temperature decreases, the radii increases. At the end of hydrogen burning, for galactic 100, 200 and $300 M_\odot$ stars with initial metallicity $Z = 10^{-6}$ their radii are $R = 20.82$, 33.40 and $43.39 R_\odot$, respectively; and for pregalactic stars with initial metallicity $Z = 10^{-9}$, $R = 12.62$, 18.61 and $24.18 R_\odot$, respectively.

On the contrary to effective temperatures, during the transition from hydrogen to helium burning, radii

slowly increase and remain almost constant during helium burning until the end when they increase again. This is, pregalactic lower metallicity stars are more compact because they are hotter than their galactic counterparts.

g) Convective core

A convective core is always present from the ZAMS to the end of the helium burning phase. Very massive Pop III stars develop a large convective core. For 100, 200 and $300M_\odot$ stars with $Z = 10^{-6}$, the convective core size at the beginning of the main sequence is $q_{cc} = 0.81$, 0.89 and 0.92, respectively. For the same stellar masses and $Z = 10^{-9}$, $q_{cc} = 0.79$, 0.88 and 0.91, respectively. The core is larger for higher metallicity.

The convective core size is larger for higher masses and increases during hydrogen burning. In fact, the studied stars are almost fully convective during hydrogen burning. At the end of this burning phase the stars contract while forming a helium core. For the masses above mentioned and metallicity $Z = 10^{-6}$, at the end of hydrogen burning, the convective core size $q_{cc} = 0.42$, 0.47 and 0.48 for 100, 200 and $300M_\odot$, respectively. For $Z = 10^{-9}$, $q_{cc} = 0.40$, 0.42 and 0.44, respectively. Then, stars with $Z = 10^{-6}$ form a helium core of $M_{He} = 42.5$, 98.3 and $142.7M_\odot$; with $Z = 10^{-9}$, the core masses are $M_{He} = 39.7$, 93.5 and $142.4M_\odot$, respectively.

Because for galactic stars with metallicity $Z = 10^{-6}$ the transition from hydrogen to helium burning is explosive, they suddenly contract, affecting momentarily their core size which rapidly increases, but then decreases while forming a helium core. That is, the exhaustion of hydrogen in the centre of the star causes a progressive contraction of the star and the shrinking of the convective core which finally vanishes when $X_c \sim 10^{-3}$. During the transition, the energy released by the star is supplied by the gravitational contraction. In the pregalactic case with $Z = 10^{-9}$ the burning transition is very smooth and the stars contract immediately forming a helium core.

During helium burning, for 100, 200 and $300M_\odot$ stars with $Z = 10^{-6}$, the convective core is $q_{cc} \sim 0.40$, 0.45 and 0.47, respectively. For $Z = 10^{-9}$, $q_{cc} \sim 0.39$, 0.43 and 0.45, respectively. That is, a carbon core mass of $M_C = 40.5$, 90.9 and $130.6M_\odot$, respectively, is formed for stars with $Z = 10^{-6}$, while for $Z = 10^{-9}$, $M_C = 39.1$, 86.4 and $134.7M_\odot$, respectively.

h) Radiation pressure

Very massive Pop III stars are dominated by radiation pressure. At the centre of the stars we have

$1 - \beta_c = 0.45$, 0.58 and 0.64 for 100, 200 and $300M_\odot$ galactic stars with metallicity $Z = 10^{-6}$. That is, the contribution of radiation pressure to the total pressure is considerable. For pregalactic stars with metallicity $Z = 10^{-9}$ we have that $1 - \beta_c = 0.45$, 0.58 and 0.64, respectively.

The contribution of the central radiation pressure increases during hydrogen burning. After the transition from hydrogen to helium burning, the central radiation pressure contribution increases and then remains almost constant.

i) The Eddington luminosity

Very massive Pop III stars evolve during hydrogen burning below the Eddington upper luminosity limit. For $Z = 10^{-6}$, at the beginning of hydrogen burning, the ratio $\Gamma = 0.60$, 0.73 and 0.79 for 100, 200 and $300M_\odot$, respectively; and for $Z = 10^{-9}$ $\Gamma = 0.60$, 0.74 and 0.80, respectively.

During hydrogen burning, this ratio increases and has a maximum close to the end of this burning phase, approximately when the helium mass fraction is 0.98 and then decreases slightly as the star reaches helium ignition. After the transition from hydrogen to helium burning, Γ increases when the helium mass fraction is approximately 0.98. Furthermore, this ratio decreases slightly but then remains almost constant during the helium burning phase.

3.3.2 Evolutionary tracks

Fig. 22 shows evolutionary tracks in the HR-diagram for 100, 150, 200, 250 and $300M_\odot$ galactic and pregalactic Pop III stars with metallicity $Z = 10^{-6}$ and 10^{-9}, respectively. The most massive stars are the hotter and most luminous. Luminosity decreases with lower metallicity. For the same stellar mass, galactic and pregalactic Pop III stars have similar luminosities. All stars settle down on the main-sequence with a high effective temperature and luminosity. During hydrogen burning all stars increase their luminosity while the helium mass fraction increase and both the central density and temperature increase.

For stars with metallicity $Z = 10^{-6}$, the transition between nuclear burnings is explosive while the star contracts. At this moment, the effective temperature and luminosity increase. Then, the luminosity remains almost constant while the effective temperature decreases. However, for different stars their luminosity and effective temperature decrease with decreasing mass and metallicity. For pregalactic stars the hydrogen to helium burning transition occurs very smoothly
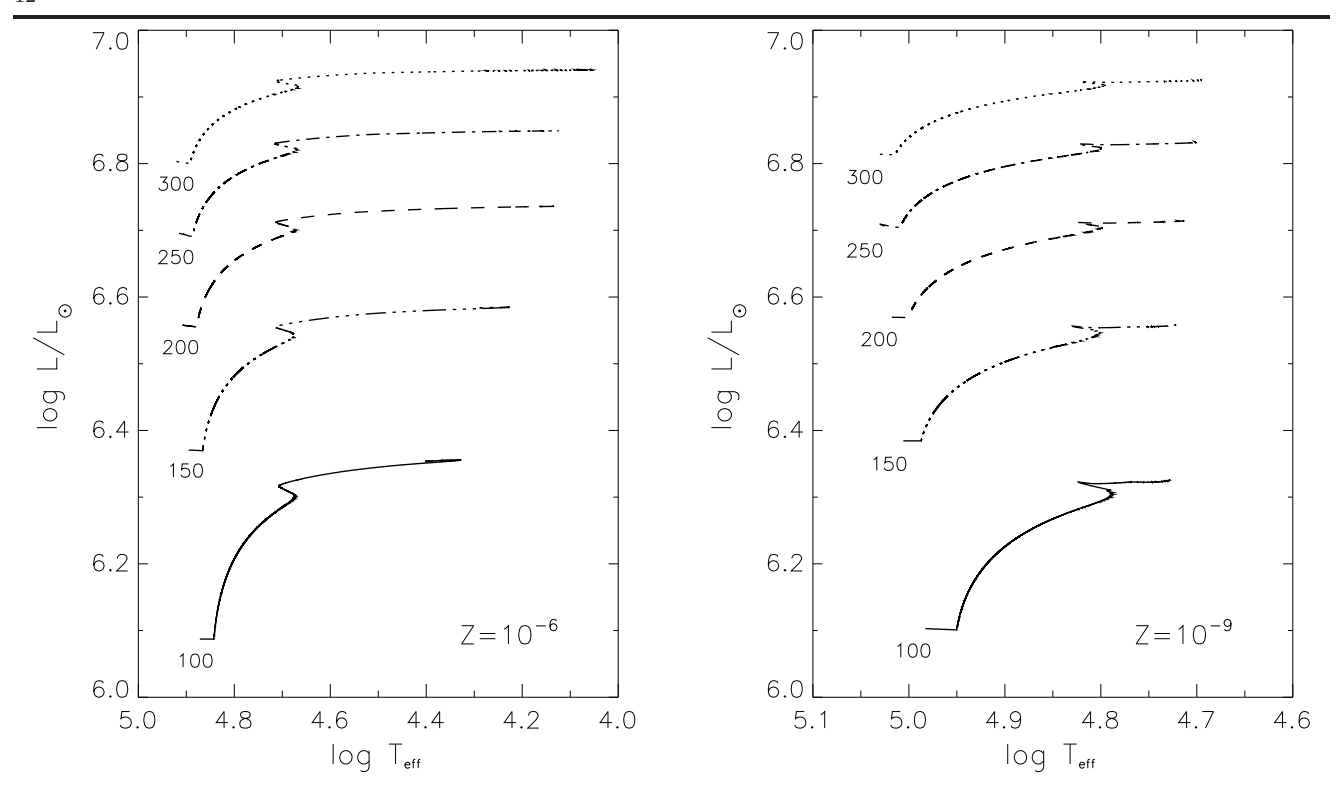
Fig. 22 Evolutionary tracks in the HR-diagram for 100, 150, 200, 250 and 300$M_\odot$ Pop III stars with metallicity $Z = 10^{-6}$ and $Z = 10^{-9}$, respectively and without mass loss during the hydrogen and helium burning phases.

because they are hotter and their central temperature is high enough to ignite helium promptly.

Galactic and pregalactic stars evolve with different lifetimes. For 100, 200 and 300$M_\odot$ galactic Pop III stars, their lifetimes during hydrogen burning are 3.07566, 2.42932 and 2.20822 megayears, respectively. For pregalactic stars, their lifetimes for the same masses are 2.87012, 2.28397 and 2.09287 megayears, respectively. During helium burning, stellar lifetimes are shorter than during hydrogen burning.

The initial hydrogen and helium burning phases take place at the blue side of the HR-diagram. When the stars evolve they move toward the red. However, the presently studied galactic and pregalactic very massive Pop III stars, evolving without mass loss and no-rotation, do not experience the asymptotic giant branch (AGB) phase. The most massive zero-metal stars tend to be cooler but the temperature remains above $\sim 10^4$ K.

The HR-diagram evolution of massive lower metallicity Pop III stars is different than for Pop I and II stars, because they do not evolve to red-giants before core collapse (Umeda et al. 2000). In the quoted range of masses used by (Castellani et al. 1983), massive zero-metal stars fail to reach the red giant region either at the hydrogen or helium burning phases.

In the Hertzprung-Russell diagram the locus of very massive Pop III stars is in the left upper part. These stars are hotter and very luminous. Pregalactic stars are hotter than galactic Pop III stars. Then, stars with lower metallicity are shifted to the left because they are bluer than the others.

k) $\rho - T$ plane

The $\rho - T$ plane describes the state of the gas in the innermost stellar regions and it is important for the diagnosis of the stellar structure and evolution. The evolution of the central conditions determine the boundaries in which the equation of state is dominated by different pressure components, i.e., ideal gas, radiation pressure or electron pressure.

According to the zones of the equation of state of an electron gas, the studied stars occupy the upper loci of a non-degenerate and non-relativistic gas. In this zone there is a boundary at which pair production could become important. Regarding the gas in thermodynamic equilibrium, these stars are dominated by radiation pressure.

The central conditions varies in the range $\log \rho_c \sim 1 - 3$ and $\log T_c = 8.0 - 8.6$ for galactic stars with $Z = 10^{-6}$. For pregalactic stars with $Z = 10^{-9}$, both the central temperature and density are higher. The

evolution of the central conditions can be described by $T_c \sim \rho_c^{1/3}$. This behaviour depends on the equation of state and it is similar for models of any metallicity.

We distinguish two regions in the $\rho - T$ plane in correspondence to the stages of gravitational contraction of stellar cores between nuclear burnings. In the second region, corresponding to helium burning, the central density and temperature increases more than during hydrogen burning.

4 Discussion

The evolutionary tracks of our massive Pop III stars are shifted to the left upper part of the HR-diagram as in Tumlinson et al. (2003) models. Then, stars evolve to the red with increasing luminosity and decreasing effective temperature. In both cases, luminosities are similar but, in the present case, final effective temperatures are slightly higher. This is probably due to the different parameters used, chemical composition and specific implementation of physical processes, e.g., convection.

a) Nuclear lifetimes

Our models are hot and luminous and have short lifetimes. For $100 M_\odot$ stars with $Z = 10^{-6}$ and 10^{-9}, their lifetimes during hydrogen burning are $\tau_{\rm H} = 3.09368$ and 2.92147 megayears, respectively. Lifetimes during helium burning are of the order of $\sim 10\%$ of their lifetime during hydrogen burning. Our results for galactic and pregalactic hydrogen burning Pop III stars are in good agreement with other authors.

For $M \gtrsim 300 M_\odot$, even metal-free stars evolve toward $T_{\rm eff} < 10^4$ K and eventually become red supergiants, as the hydrogen burning shell becomes more active with increasing stellar mass (Baraffe et al. 2001). In the present work, the most massive metal-free stars tend to be cooler and likely could become red supergiants. However, for a helium mass fraction equal to ~ 0.01, they maintain high effective temperatures. In all cases, stars do not reach low effective temperatures. Evolving stars without mass loss and with no-rotation, fail to reach the AGB phase. At the end of helium burning, the studied galactic stars are hotter than $\log T_{\rm eff} \sim 4.0$ and pregalactic stars are hotter than $T_{\rm eff} \sim 4.6$.

b) Nuclear energy generation

The peculiar behaviour of low metallicity stars was first pointed out by Ezer (1961) and their structure during hydrogen and helium burning has been investigated by several authors.

According to the results presented here the stars begin to settle down on the main-sequence with higher initial central temperatures of order $\log T_c \sim 8$. Then, the onset of the 3α reaction occurs at earlier stages of hydrogen burning. This is because the 3α reaction requires a much higher temperature than the pp-chains and ignites at the beginning of the hydrogen burning phase. In the present models, after a brief initial period of 3α burning, a trace amount of heavy elements has been formed. Then, the stars expand and follow the CNO-cycles.

In Fig. 23 the nuclear energy generation as function of the temperature is shown, and Fig. 24 shows this energy generation during hydrogen burning for both galactic and pregalactic Pop III stars.

c) Convective core size

In their models, Marigo et al. (2001) found that if the convective core grows, it eventually reaches the H-shell and engulfs some hydrogen-rich material, which is rapidly burnt via the CNO-cycles. This causes a flash that expands the core, so that central helium burning weakens and the convective core recedes temporarily (in mass). After the flash has occurred, the convective core starts growing again.

In the present models, the same picture takes place for galactic Pop III stars but it does not in the pregalactic case. In this case, the central temperature at the transition of nuclear burnings is higher than in the first one.

Hydrogen exhaustion in the centre of the star causes a progressive contraction of the star and the shrinking of the convective core which finally vanishes when $X_c \sim 10^{-3}$, so that no standard overall contraction phase is found (Castellani et al. 1983). A maximum in the energy released by gravity occurs during this burning phase, when $X_c = 10^{-9}$, and 59% of the energy released by the star is supplied by contraction. Ignition of the full triple-α cycle is only slightly delayed with respect to hydrogen burning ignition in a shell, and once again the gravitational contraction supplies energy to the star. Once the 3α chain has become fully efficient, a convective core is again developed.

For the present work, pregalactic Pop III stars have higher temperatures than galactic stars allowing a soon ignition of the 3α reactions. Then the transition from hydrogen to helium burning is smooth because the convective core does not vanish.

d) Eddington luminosity

Stellar models may become gravitationally unbound, i.e., the rate of energy outflow at the surface exceeds the corresponding Eddington luminosity.
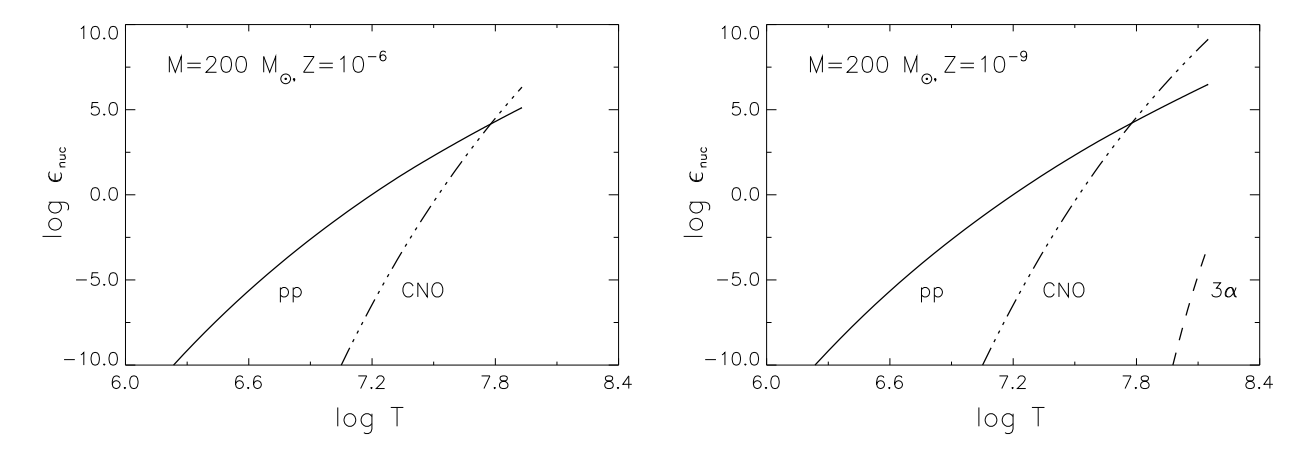
Fig. 23 Main sequence nuclear energy generation rate as function of the temperature for $200 M_\odot$ galactic (left panel), and pregalactic (right panel) Pop III stars, with metallicity $Z = 10^{-6}$ and $Z = 10^{-9}$, respectively.

Fig. 24 Main sequence nuclear energy generation rate as function of the hydrogen mass fraction for $200 M_\odot$ galactic (left panel), and pregalactic (right panel) Pop III stars, with metallicity $Z = 10^{-6}$ and $Z = 10^{-9}$, respectively.
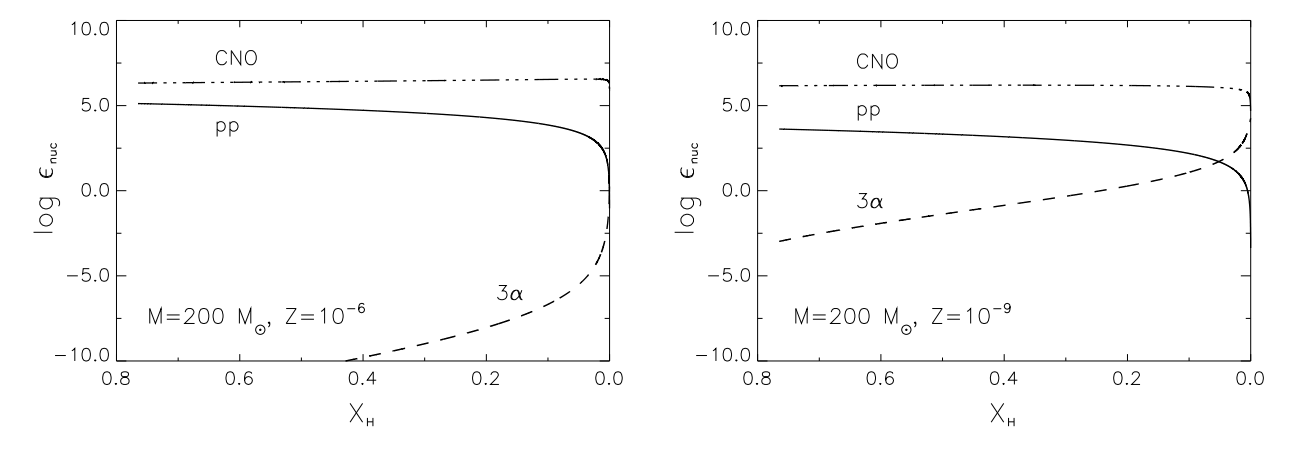
In the present models, the Eddington Γ factor is calculated by estimating the ratio between the current stellar luminosity and the Eddington luminosity. In both the hydrogen and helium burning phases, the studied cases of 100, 200 and $300M_\odot$ galactic and pre-galactic Pop III stars evolve below the upper Eddington luminosity limit. During hydrogen burning, the Γ factor increases, reaches a maximum toward the end of this burning phase and then decreases. The most massive stars evolve during the helium burning phase closest to the Eddington limit.

5 Conclusions

For the present work a large number of ZAMS models have been calculated showing the main physical variables as function of the mass, and the metallicity. As the mass increases, ZAMS stars get bigger, brighter, and less dense. Pop III stars get very hot and compact as metallicity decreases.

When metal-free stars settles down on the main-sequence, they have smaller radii, hotter cores, and higher effective temperatures than metal-enriched stars. Like their counterparts, lower metallicity stars become systematically cooler, larger and more luminous over their hydrogen burning lifetimes. The most massive stars have shorter lifetimes than less massive stars.

To study their properties and internal structure, stellar structure models on the main sequence have been calculated, emphasizing the case of metal-free stars which are compared with their Pop I and II counterparts. Pop III stars are more centrally condensed, denser and hotter. On the main sequence their different internal regions are always below the upper Eddington luminosity limit.

The most important feature of the metal-free models is the high temperature they maintain in their photosphere. These stars have a high ionizing photon production rate. The ionization caused by these stars is a direct result of their high effective temperatures. For $M > 100M_\odot$, the studied metal-free stars have effective temperatures $T_{\rm eff} \sim 10^5$ K. Consequently, they are very efficient at producing photons capable of ionizing hydrogen and helium. According to Bromm, Kudritzki and Loeb (2001), very massive Pop III stars might have played a significant role in the IGM reionization of hydrogen and helium at high redshifts.

Nuclear burning proceeds in a non-standard way. For stars with no metals, the pp-chains and the CNO-cycles do not provide enough energy to support the star, so when it reaches the main sequence keeps contracting until the 3α process starts to operate, halts the contraction and in a very small time produces enough CNO elements so that the energy from the CNO-cycle is capable of supporting the star, which expands and settles down to the main sequence. The stars maintain core temperatures in excess of $T_{\rm c} > 10^8$ K which are high enough for the simultaneous occurrence of the pp-chains, the CNO-cycles and helium burning via the 3α process.

For these stars, the radiative opacity in their envelopes is reduced, and their core temperature is high, then the *first stars* are hotter and smaller than metal-enriched stars. On the other hand, the opacity of stellar matter is reduced at low metallicity, permitting steeper temperature gradients and more compact configurations at the same mass.

Very massive ($M \gtrsim 100M_\odot$) galactic and pre-galactic Pop III stars develop large convective cores with important helium core masses $M_{\rm He} \sim 40M_\odot$. These quantities are important for explosion calculations (Umeda et al. 2000) and synthetic derivation of the SN yields (Portinari et al. 1998). Semiconvection does not greatly affect the stellar structure during the main-sequence phase. However, during the shell hydrogen burning and helium burning phases, it plays a significant role, and the evolutionary results depends on the adopted criterion and the input physics of the models (Chiosi and Maeder 1986).

We have calculated evolutionary models for lower metallicity very massive Pop III stars. The evolution of these stars is similar to that of metal enriched stars but now the evolutionary tracks are shifted to the left of the HR-diagram, i.e. the models are bluer than their metal enriched counterparts. This is because massive Pop III stars are hotter and very luminous. Pregalacic stars are denser and hotter than galactic Pop III stars. However, during their evolution these stars are more luminous than the first ones.

During the hydrogen burning phase, very massive galactic and pregalactic Pop III stars evolve almost fully convective. They form a large core with a different structure depending on metallicity. Very massive stars are dominated by radiation pressure and electron scattering. As a consequence of the high radiation pressure, the convective core tends to be larger at higher masses and to expand as the star evolves.

Because the stars radiate near the Eddington limit, radiation pressure due to electron scattering opacity can become substantial. For pregalactic Pop III stars, with the metallicity $Z = 10^{-9}$ considered in this work, they develop a helium core $M_{\rm He} = 39.7$, 93.5 and $142.4M_\odot$, corresponding to initial stellar masses of 100, 200 and $300M_\odot$, respectively. Then, according to Fryer et al. (2001) and Heger and Woosley (2002), these stars

will likely explode by pair-instability supernovae for the 200 and $300M_\odot$ cases or collapse into black holes for the $100M_\odot$ case. However, $M < 130M_\odot$ stars could explode like hypernovae.

The present evolutionary models have been calculated without mass loss and with ro-rotation, in accordance with other existing points of view. However, the uncertain role of mass loss can be viewed as one of the major systematic uncertainties remaining in the study of metal-free stars. In subsequent papers we will extend the present study to mass losing and rotating models.

References

Abel, T., Bryan, G.L., Norman, M.L.: Astrophys. J.**540**, 39 (2000)

Abel, T., Bryan, G.L., Norman, M.L.: Science **293**, 93 (2002)

Angulo C., Arnould M., Rayet M. et al: Nucl. Phys. A **656** 3 (1999)

Bahena, D.: PhD Thesis, UK Praha (2006)

Bahena, D., Klapp, J.: Rev. Mex. Fís. S **53**, 48 (2007)

Baraffe, I., Heger, A., Woosley, S.E.: Astrophys. J.**550**, 890 (2001)

Barkat, Z., Rakavy, G., Sack, N.: Phys. Rep. **349**, 125 (1967)

Bond, H.E.: Astrophys. J.**248**, 606 (1981)

Bond, J.R., Arnett, W.D., Carr, B.J.: Astrophys. J.**280**, 825 (1984)

Bromm, V, Larson, R.: Annu. Rev. Astron. Astrophys.**42**, 79 (2004)

Bromm, V, Coppi, P.S., Larson, R.: Astrophys. J.**527**, L5 (1999)

Bromm, V, Kudritzki, R.P., Loeb, A.: Astrophys. J.**552**, 464 (2001)

Bromm, V, Coppi, P.S., Larson, R.: Astrophys. J.**564**, 23 (2002)

Bromm, V, Yoshida, N., Hernquist, L.: Astrophys. J.**596**, L135 (2003)

Carr, B.J.: Nature**326**, 829 (1987)

Carr, B.J.: Annu. Rev. Astron. Astrophys.**32**, 531 (1994)

Castellani, V.: in *The First Stars*, Proc. MPA/ESO Workshop, eds. A. Weiss, T.G. Abel and V. Hill, Springer, p.85 (2000)

Castellani, V., Chieffi, A., Tornambé, A.: Astrophys. J.**272**, 249 (1983)

Caughlan, G.R., Fowler, W.A.: Atomic Data and Data Nuclear Tables **40**, 283 (1988)

Caughlan, G.R., Fowler, W.A., Harris, M.J., Zimmermann, B.A.: At. Data Nucl. Data Tables **32**, 197 (1985)

Cayrel, R.: Astron. Astrophys.**168**, 81 (1986)

Cayrel, R.: Astron. Astrophys. Rev.**7**, 217 (1996)

Cen, R.: Astrophys. J.**591**, 12 (2003)

Chiosi, C., Maeder, A.: Annu. Rev. Astron. Astrophys.**24**, 329 (1986)

Christy, R.: Astrophys. J.**144**, 108 (1966)

Dodelson, S., Jubas, J.M.: Astrophys. J.**439**, 503 (1995)

Ezer, D.: Astrophys. J.**133**, 159 (1961)

Ferrara, A.: Astrophys. J.**499**, L17 (1998)

Fryer, C.L., Woosley, S.E., Heger, A.: Astrophys. J.**559**, 372 (2001)

Gnedin, N.Y., Ostriker, J.P.: Astrophys. J.**486**, 581 (1997)

Haiman, Z., Loeb, A.: Astrophys. J.**483**, 21 (1997)

Heger, A., Woosley, S.E.: Astrophys. J.**567**, 532 (2002)

Heger, A., Fryer, C.L., Woosley, S.E., Langer, N., Hartmann, D.H.: Astrophys. J.**591**, 288 (2003)

Iglesias C.A., Rogers F.J. Astrophys. J.**412**, 752 (1993)

Klapp, J.: PhD Thesis, Oxford University (1981)

Klapp, J.: Astrophys. Space Sci.**93**, 313 (1983)

Klapp, J.: Astrophys. Space Sci.**106**, 215 (1984)

Klapp, J., Bahena, D., Corona-Galindo, M.G., Dehnen, H.: in *Gravitation and Cosmology*, eds. A. Macías, C. Lämmerzahl and D. Nuñez, Mellville N.Y., AIP Conf. Proc. **758**, p. 153 (2005)

Kogut, A., Spergel, D.N., Barnes, C., et al.: Astrophys. J. Suppl. Ser.**148**, 161 (2003)

Kudritzki, R.P.: in *The First Stars*, Proc. MPA/ESO Workshop, eds. A. Weiss, T. Abel and V. Hill, Springer, p.127 (2000)

Kudritzki R.P.: Astrophys. J.**557**, 389 (2002)

Larson, R., Bromm, V.: Sci. Am. **14**, 4 (2004)

Marigo, P., Girardi, L., Chiosi, C., Wood, P.R.: Astron. Astrophys.**371**, 152 (2001)

Meynet, G., Maeder, A.: Astron. Astrophys.**390**, 561 (2002)

Miralda-Escudé, J., Haehnelt, M., Rees, M.J.: Astrophys. J.**230**, 1 (2000)

Nakamura, F., Umemura, M.: Astrophys. J.**548**, 19 (2001)

Ober, W.W., El Eid, M.F., Fricke, K.J.: Astron. Astrophys.**119**, 61 (1983)

Omukai, K., Palla, P.: Astrophys. J.**589**, 677 (2003)

Ostriker, J.P., Gnedin, N.Y.: Astrophys. J.**472**, L63 (1996)

Portinari, L., Chiosi, C., Bressan, A.: Astron. Astrophys.**334**, 505 (1998)

Rogers F.J., Iglesias C.A.: Astrophys. J. Suppl. Ser.**79**, 603 (1992)

Schaerer, D.: Astron. Astrophys.**382**, 28 (2002)

Sokasian, A., Abel, T., Hernquist, L., Springel, V.: Mon. Not. R. Astron. Soc.**344**, 607 (2003)

Tegmark, M., Silk, J., Rees, M. J., Blanchard, A., Abel, T., Palla, F.: Astrophys. J.**474**, 1 (1997)

Tumlinson, J., Shull, M.J.: Astrophys. J.**528**, L65 (2000)

Tumlinson, J., Shull, J. M., Venkatesan, A.: Astrophys. J.**584**, 608 (2003)

Tumlinson, J., Venkatesan, A., Shull, J. M.: Astrophys. J.**612**, 602 (2004)

Umeda, H., Nomoto, K., Nakamura, T.: in *The First Stars*, Proc. MPA/ESO Workshop, eds. A. Weiss, T. Abel and V. Hill, Springer, p.150 (2000)

Umeda, H., Nomoto, K.: Astrophys. J.**565**, 385 (2002)

Visniac, E.T.: Astrophys. J.**322**, 597 (1987)

Yoshida, N., Bromm, V., Hernquist, L.: Astrophys. J.**605**, 579 (2005)

Wyithe, J.S.B., Loeb, A.: Astrophys. J.**586**, 693 (2003)